Thermally activated flux motion in a one-dimensional Josephson-junction array with self-inductances

H. P. Fischer, T. Wolf, and W. Dieterich
Fakultät für Physik, Universität Konstanz, D-78434 Konstanz, Germany

A. Majhofer
Institute of Experimental Physics, Warsaw University, PL-00 681 Warszawa, ul. Hoża 69, Poland
(Received 6 July 1995)

We study relaxation of magnetic flux in a one-dimensional network of resistively shunted Josephson junctions. Magnetic fields due to the currents induced in the system are taken into account via self-inductance coefficients. A master equation is derived that describes the stochastic motion of flux quanta among the different plaquettes of the network. Space- and time-dependent flux profiles are calculated within mean-field theory and also by a continuous-time Monte Carlo algorithm. The relevance of our results for the description of flux creep experiments in strongly inhomogeneous superconductors is pointed out. [S0163-1829(96)08441-X]

I. INTRODUCTION

High-temperature superconductors are known to be characterized by short coherence lengths, with the important effect that structural inhomogeneities in the material generally lead to an inhomogeneous superconducting state. In recent years, several authors have advanced the idea that strongly inhomogeneous superconductors may be regarded as networks of Josephson weak links connecting islands of material with ideal intrinsic properties.[1–3] Under this point of view a considerable amount of work has been devoted to the study of Josephson networks,[3–14] with the conclusion that at least some of the important macroscopic properties of high-T_c materials, including magnetic properties and current-voltage characteristics, can qualitatively be understood on this basis. In particular, a fairly realistic description of magnetic hysteresis effects, ac susceptibilities, and flux patterns in bulk samples[10,11] and thin films[12] has been achieved, using network models where inductance effects adapted to the sample geometry were taken into account. Similar models have also been used to analyze the form of a single, extended Josephson vortex[13] as well as giant Shapiro steps in large, artificial arrays of junctions.[14]

In a Josephson network pinning forces naturally arise from the discreteness of the system. For large pinning a critical state can be defined, whose coarse-grained properties are similar to conventional critical state models. For a system in a critical state the question arises how the magnetization relaxes when thermal fluctuations are taken into account, and how this relaxation compares with flux creep experiments on high-T_c samples. Thermal fluctuations and magnetic relaxation in a superconducting loop containing a single Josephson weak link were discussed recently by Niewenhuizen and Pankert.[15] Here we extend both the idea of these authors and our previous work[10,11] by studying a Josephson array including thermal noise. This allows us to relate the overall relaxation to the temporal evolution of the underlying flux patterns. Such an investigation should be useful in view of the fact that spatially resolved flux creep phenomena are becoming accessible to experiment.[16]

Magnetic relaxation in high-T_c materials is known to be large and often departs from the logarithmic decay law, $M(t)\sim\ln t$ implied by the conventional flux-creep model.[1,17–21] In order to account for these observations, several new concepts have been proposed, such as flux motion under the influence of a distribution of activation barriers,[22] collective flux creep,[23,24] or the dynamics of flux near a transition from a vortex liquid to a vortex glass.[25] The model presented below is clearly simplified as it ignores any effect of disorder. Instead, it focuses on thermally activated flux motion in the presence of magnetic interactions in a regular Josephson network. For the present purpose, we confine ourselves to the case of strong pinning, where the full stochastic dynamics of the network can be approximated by a master equation that describes a discrete ''hopping'' process of flux quanta among the different plaquettes. For simplicity, we consider a one-dimensional finite chain of superconducting loops in a perpendicular magnetic field, which in an averaged way may represent the behaviour of a sample of slab geometry. We find that only under certain restricted conditions the conventional logarithmic decay law for the total magnetization applies, and that a nonlogarithmic behaviour becomes especially pronounced in cases where the maximum superconducting current I_0 in a junction depends on the local magnetic field. In many respects our results are similar to the experimental findings by Svedlindh *et al.*,[19,26] who investigated magnetic relaxation processes in ''extreme'' type-II superconductors.

This paper is organized as follows. In Sec. II we give a short account of our model and explain the character of the adopted approximations. Numerical results obtained within mean-field theory are discussed in Sec. III, and are compared with experimental data. Section IV contains examples of solutions to our master equation reached within a continuous-time Monte Carlo algorithm. These examples corroborate the assumptions made in Sec. II and in addition indicate that magnetic relaxation at low temperatures proceeds through a series of ''avalanches.''

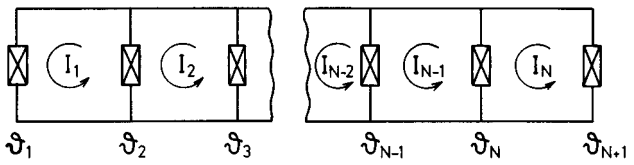

FIG. 1. Schematic view of a one-dimensional network of Josephson junctions with indicated elementary current loops I_i and gauge-invariant phase differences ϑ_i across elements which consist of an ideal Josephson junction in parallel with a normal resistance R (RSJ model). A self-inductance L is associated with each plaquette. The external field is perpendicular to the network.

II. STOCHASTIC JOSEPHSON NETWORK AND MEAN-FIELD APPROXIMATION

We start our analysis with the formulation of the Langevin dynamics for a one-dimensional Josephson array depicted in Fig. 1. The array consists of N identical elementary loops subject to a perpendicular external field. Each junction is characterized by its maximal superconducting current I_0, its normal resistance R, and the gauge-invariant phase difference ϑ,

$$\vartheta = \Delta\varphi - \frac{1}{\phi_0}\int \mathbf{A}\, d\mathbf{l}, \tag{1}$$

where $\Delta\varphi$ is the difference of phases of the order parameters in superconductors forming the link, $\mathbf{A}$ is the vector potential, and the integral is taken across the junction, while $\phi_0 = h/(4\pi e)$. Additionally, each junction is resistively shunted by normal currents and the total current through the junction i $(i=1,\ldots,N+1)$ is then given by

$$I_i - I_{i-1} = I_0 \sin\vartheta_i + \frac{\phi_0}{R}\frac{d\vartheta_i}{dt} + I_i^f(t). \tag{2}$$

In writing Eq. (2) we took into account Josephson's equations, the parametrization of currents as shown in Fig. 1 and a Nyquist noise term $I_i^f(t)$ associated with the normal resistance R. The ensemble average of the noise current and its correlation function satisfy the standard relations:[27]

$$\langle I_i^f(t)\rangle = 0 \tag{3}$$

and

$$\langle I_i^f(t) I_j^f(t')\rangle = \frac{2}{R} k_B T \delta_{ij}\delta(t-t'). \tag{4}$$

Equation (1) implies that ϕ_i, the total magnetic flux through the plaquette i $(i=1,\ldots,N)$, is given by

$$\frac{\phi_i}{\phi_0} = \vartheta_i - \vartheta_{i+1}. \tag{5}$$

Finally we assume[10,12]

$$\phi_i = \phi_{\rm ext} - L I_i, \tag{6}$$

with $\phi_{\rm ext}$ denoting the external flux and L the self-inductance coefficient of a plaquette. The neglect of more general inductance coefficients may be justified for samples of slab geometry in a parallel magnetic field, if we assume that only screening currents perpendicular to the field are important, and that the current distribution in planes parallel to the slab is uniform. An averaged description of such a system then leads to the one-dimensional system of Eqs. (2)–(6), where i is the coordinate perpendicular to the slab; cf. also Ref. 11. Elimination of I_i and ϕ_i leads to a system of Langevin equations for the phases ϑ_i, which can be written in the form

$$\frac{\phi_0^2}{R}\frac{d\vartheta_i}{dt} = -\frac{\partial V}{\partial\vartheta_i} + \phi_0 I_i^f(t), \tag{7}$$

where the potential is given by

$$V = I_0\phi_0\left[\frac{1}{2\beta}\sum_{i=1}^{N}\left(\frac{\phi_{\rm ext}}{\phi_0} - \vartheta_i + \vartheta_{i+1}\right)^2 - \sum_{i=1}^{N+1}\cos\vartheta_i\right]. \tag{8}$$

Here we have introduced the dimensionless parameter $\beta = LI_0/\phi_0$ which measures the pinning strength of a single plaquette. In fact, β determines the maximum flux gradient that can be maintained in a stationary state in the absence of noise,

$$|\phi_i - \phi_{i-1}|_{\max} = \beta\phi_0, \tag{9}$$

which is obvious from Eqs. (6) and (2).

One typical problem is to study magnetic relaxation from a zero-field-cooled sample which corresponds to initial conditions $\vartheta_i(t=0)=0$. In the case of strong pinning ($\beta\gg1$), which is most relevant to strongly inhomogeneous superconductors, relaxation will occur via two distinctly different processes with different time-scales. Initially, there will be fast relaxation on a time scale $t_{\rm micro}\approx L/R$ due to the action of the systematic forces $-\partial V/\partial\vartheta_i$ in Eq. (7) until a state is reached which would be stationary at $T=0$, i.e., in the absence of noise. As shown previously[10] this state for $\beta\gg1$ is similar to the Bean critical state with linear flux profiles determined by the condition (9). The subsequent decay of such profiles due to the presence of noise will be the main objective of our investigation here. In principle one could employ Langevin-dynamics simulations. However, it turns out in our present problem that this technique is only of limited practical use. Focusing on low temperatures, we are faced with exceedingly long relaxation times, to be derived from an elementary time for escape over pinning barriers of strength $2I_0\phi_0$, see Eq. (8), $t_{\rm escape}\approx\exp(2I_0\phi_0/k_BT)t_{\rm micro}\gg t_{\rm micro}$. (Rough estimates show that for sintered samples $t_{\rm micro}\sim10^{-12}$ s.[11] This value has to be compared with $\sim10^4$ s as a typical time scale for flux creep measurements.) Apart from the early stages of the relaxation it is then clearly appropriate to adopt a coarse-grained description in terms of a master equation, which describes the time evolution of discrete configurations defined through the metastable minima of the potential (8). An approach of this type was proposed before by Niewenhuizen and Pankert[15] for the case of a single superconducting loop, and will be generalized here to our problem of a one-dimensional array. When $\beta\gg1$, the system is found most of the time in states with all phases close to integer multiples of 2π,

$$\vartheta_i \simeq 2\pi l_i \tag{10}$$

as a consequence of the last term in Eq. (8). This implies, of course, that the system has already relaxed for a sufficiently long time, that the actual currents through all the junctions be substantially smaller than I_0. By Eq. (5), the flux ϕ_i then becomes quantized, $\phi_i \simeq (2\pi\phi_0)n_i$, where the number n_i of flux quanta through the ith plaquette is given by

$$n_i = l_i - l_{i+1}. \tag{11}$$

The increase (or decrease) of ϑ_i by 2π corresponds to the motion of one flux quantum from plaquette $i-1$ to i (or vice versa). The barriers to be overcome in these processes are calculated as

$$\begin{aligned}\Delta E_i^{\pm} &\simeq V(\ldots,\vartheta_i \pm \pi,\ldots) - V(\ldots,\vartheta_i,\ldots) \\ &\simeq 2I_0\phi_0[1 \pm \pi^2(n_i - n_{i-1})/\beta]\end{aligned} \tag{12}$$

and the corresponding transition rates are given by

$$W^{\pm}(n_i, n_{i-1}) = \nu \exp(-2/T^*)\exp[\mp\alpha(n_i - n_{i-1})], \tag{13}$$

where $\nu = \beta R/2\pi L$ and $\alpha = 2\pi^2/\beta T^*$ with

$$T^* = \frac{k_B T}{I_0\phi_0}. \tag{14}$$

In writing Eq. (13) we assumed $\Delta E_i^{\pm} \gg k_B T$ and used the standard escape rates in the overdamped (Smoluchowski) limit.[28]

Furthermore let us remark that the dependence of the energy barrier on occupation numbers as given by Eq. (12) corresponds to the leading contribution in an expansion in powers of β^{-1}. Higher order terms in Eq. (12) due to corrections $O(\beta^{-2})$ in Eq. (10) would involve the flux in next-nearest-neighbor or higher-neighbor plaquettes.

At this stage we can formulate a master equation that describes jumps of individual flux quanta between neighboring plaquettes:[28]

$$\begin{aligned}\frac{d}{dt}P(n_1,\ldots,n_N;t) = \sum_{i=1}^{N} \{&P(\ldots,n_{i-1}+1,n_i-1,\ldots)W^+(n_i-1,n_{i-1}+1) + P(\ldots,n_i-1,n_{i+1}+1,\ldots)W^-(n_{i+1}+1,n_i-1) \\ &- P(\ldots,n_i,\ldots)[W^+(n_{i+1},n_i) + W^-(n_i,n_{i-1})]\},\end{aligned} \tag{15}$$

where the external flux enters via the definitions $n_0 = n_{N+1} = n_{\rm ext} = \phi_{\rm ext}/2\pi\phi_0$. More phenomenological schemes for thermally activated forward and backward hopping of flux quanta during flux penetration into the sample were described before by several authors.[29–31] Equation (15), however, represents a coherent stochastic description for the temporal *and* spatial relaxation of flux including magnetic interactions in the system. The discrete hopping processes which we have assumed appear physically meaningful as long as $\Delta E_i^{\pm} \gg k_B T$, or

$$2 - \frac{2\pi^2}{\beta}|n_i - n_{i-1}| \gg T^*. \tag{16}$$

Our primary aim is now to calculate from Eq. (15) the time-dependent average occupation numbers

$$\langle n_i \rangle = \sum_{\{n_i\}} n_i P(n_1,\ldots,n_N;t) \tag{17}$$

from which we obtain the average total number of flux quanta

$$n_{\rm tot}(t) = \sum_{i=1}^{N} \langle n_i \rangle, \tag{18}$$

which is related to the total magnetization by $M(t) = 2\pi\phi_0(n_{\rm tot}(t) - N n_{\rm ext})$.

In a first step we shall use mean-field theory, where it should be noted that mean-field ideas have already been invoked before in mapping an acutal experimental situation to our one-dimensional model [see the above discussion after Eq. (6)]. Nevertheless it appears interesting also to perform numerical simulations and to compare them with the mean-field results, which will be done in Sec. IV. From the master equation (15) together with Eq. (13) the time derivative of $\langle n_i \rangle$ is readily calculated in terms of averages of the type $\langle \sinh \alpha(n_{i+1} - n_i) \rangle$. Mean-field theory now corresponds to the factorization

$$\left\langle \prod_i n_i \right\rangle \simeq \prod_i \langle n_i \rangle, \tag{19}$$

with the result

$$\frac{d\langle n_i \rangle}{d\tau} = J_i - J_{i-1}, \tag{20}$$

where the current of magnetic flux is given by

$$J_i = 2\exp(-2/T^*)\sinh\alpha(\langle n_{i+1}\rangle - \langle n_i \rangle) \tag{21}$$

and $\tau = \nu t$ is a dimensionless time. Any linear flux profile obviously is stationary under these mean-field equations. The time evolution of a profile that, for example, corresponds to a Bean critical state in a zero-field-cooled sample therefore must start out in a region located near the penetration depth.

In comparing this type of theory to experiments, it seems important to consider a phenomenological extension of the model defined by Eqs. (7) and (8) by taking into account a dependence of the maximum Josephson current on the local magnetic field. In our model, the local field B_i acting on the ith junction may be written in terms of an average over the

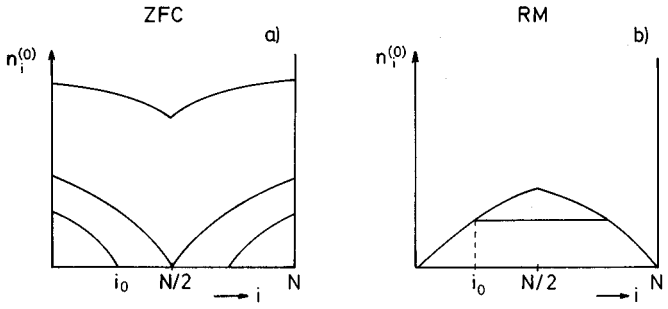

FIG. 2. Schematic representation of initial flux distributions $n_i^{(0)}$ determined by Eq. (24). The penetration depth is denoted by i_0. (a) Zero-field-cooled (ZFC) sample for external fields $n_{\rm ext}>n_K^*$, $n_{\rm ext}=n_K^*$, and $n_{\rm ext}<n_K^*$ (from above) and (b) remanent flux of a field-cooled sample (RM). In this case all profiles for $n_{\rm ext}\geqslant n_K^*$ coincide (upper curve), whereas for $n_{\rm ext}<n_K^*$ a plateau of constant flux appears (lower curve).

magnetic flux in the two adjacent plaquettes. Following the standard Kim model, the maximum Josephson current through the ith junction is assumed to be of the form[32]

$$I_{0i}=\frac{I_0}{1+\Lambda|n_i+n_{i-1}|/2}, \tag{22}$$

where we again expressed the local flux in terms of the occupation numbers n_i, and $\Lambda\geqslant 0$ is a parameter [cf. Ref. 11 for a discussion of the applicability of Eq. (22) as an effective maximum Josephson current in the description of high-T_c ceramics and for references to the relevant experimental work]. To obtain equations of motion in this case, we merely have to replace β in the expression for the systematic force in Eq. (7) by $\beta_i=LI_{0i}/\phi_0$ and to use again Eq. (5). Note, however, that a potential $V(\ldots,\vartheta_i,\ldots)$ does not exist in the case $\Lambda\neq 0$. Finally, our mean-field equations take the form of Eq. (20), where the flux current is now given by

$$J_i(\Lambda)=2\sinh\,\alpha(\langle n_{i+1}\rangle-\langle n_i\rangle)\exp\left[\frac{-2/T^*}{1+\Lambda|\langle n_{i+1}\rangle+\langle n_i\rangle|/2}\right], \tag{23}$$

with $J_i(0)=J_i$.

In the next section we discuss numerical results obtained from these equations. (As far as the temperature dependence of our results is concerned, we ignore the temperature dependence of I_0, which in a more realistic model should follow the Ambegaokar-Baratoff formula.[33,34]) Some analytical considerations based on the continuum form of Eq. (20) are presented in the Appendix.

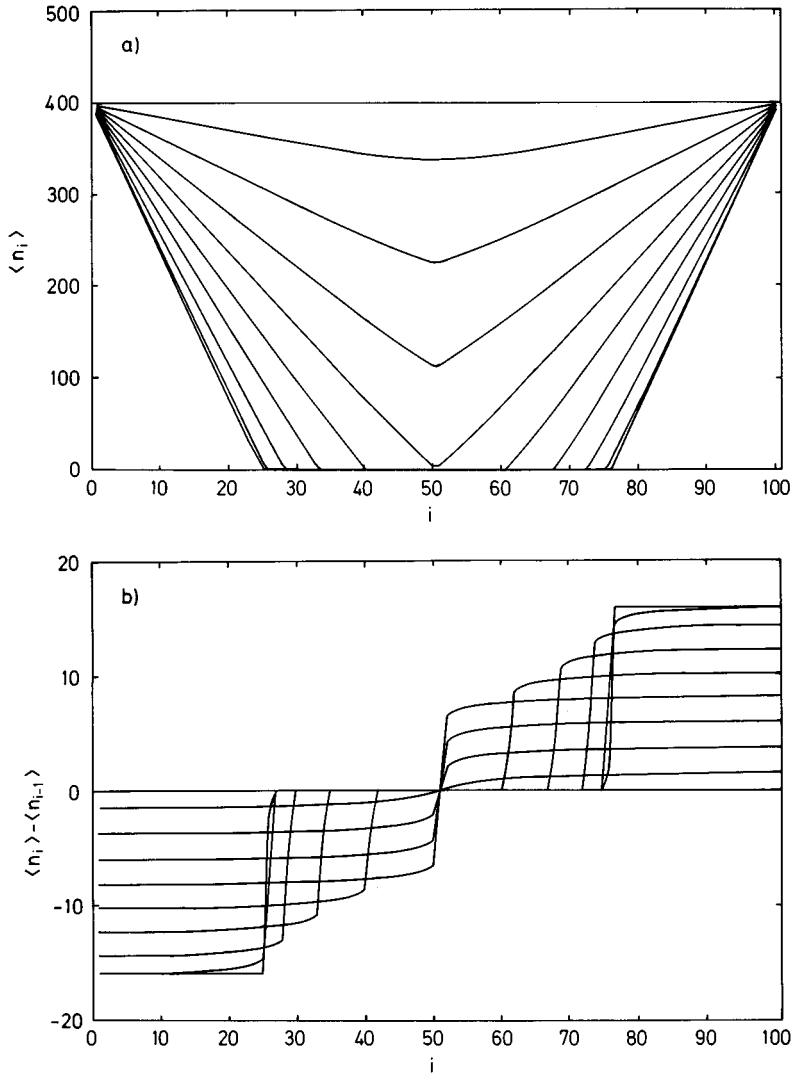

FIG. 3. Results from mean-field approximation for the ''Bean model'' ($\Lambda=0$). (a) Time evolution of a ZFC flux profile and (b) the corresponding slopes, which are proportional to the local currents. The other parameters are $\beta=100$, $T^*=0.1$, and $n_{\rm ext}=400\approx n_B^*/2$. Time steps τ_k are taken as $\ln\tau_k=(40/9)k$; $k=0,\ldots,9$.

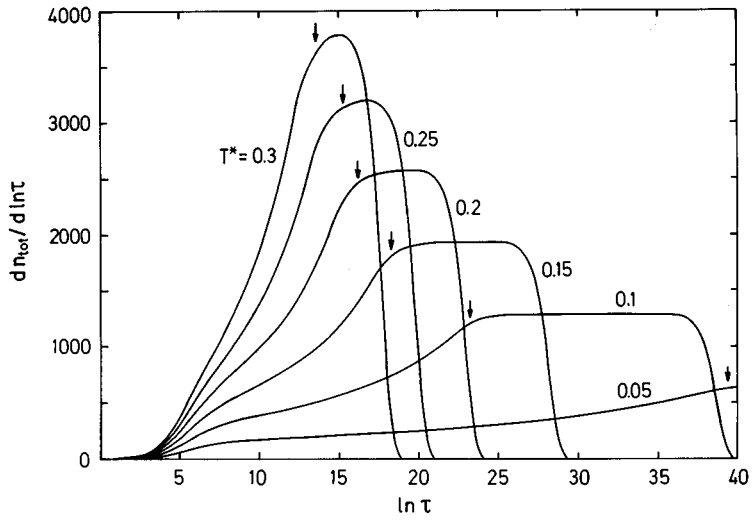

FIG. 4. ZFC creep rates within mean-field approximation for different temperatures, where $\Lambda=0$ (''Bean model''), $\beta=100$, and $n_{\rm ext}=400 \approx n_B^*/2$. The arrows indicate the time τ^* (see text).

III. NUMERICAL SOLUTIONS OF MEAN-FIELD EQUATIONS

The system of Eqs. (20) is solved numerically for $N=100$ and $\beta=100$, assuming different temperatures T^* and external fields $n_{\rm ext}$. (This value for β is of the order of magnitude estimated for ceramic superconductors.[11]) Two standard situations are considered: (a) relaxation of magnetic flux entering a zero-field-cooled (ZFC) sample and (b) relaxation of remanent flux (RM) trapped in a field-cooled system after the external field has been switched off. First we generate the corresponding critical state distributions which build under the intrinsic dynamics, in the absence of noise. The appropriate stationary solutions of our original equations (7) with $I_i^{\rm f}(t)=0$ are obtained by requiring that flux gradients are determined by the maximal Josephson currents I_{0i}; see Eq. (22). In terms of our variables $\langle n_i\rangle$ this leads to the condition $\langle n_i(\tau=0)\rangle = n_i^{(0)}$, where in the penetrated region $n_i^{(0)}$ is determined by

$$|n_{i-1}^{(0)}-n_i^{(0)}|=(\beta/2\pi)[1+\Lambda|n_{i-1}^{(0)}+n_i^{(0)}|/2]^{-1}. \quad (24)$$

From that we obtain the familiar Bean or Kim profiles in cases $\Lambda=0$ or $\Lambda\neq 0$, respectively. The two situations described above are depicted schematically in Fig. 2. As usual, we introduce the external flux n^* where flux starts to penetrate the entire sample. In the ''Bean model,'' we have $n_B^*=(\beta/2\pi)N/2$, whereas in the ''Kim model'' $n_K^*<n_B^*$.

The distributions $n_i^{(0)}$ are in turn used as initial conditions in our mean-field equations for some finite temperature $T\neq 0$, from which we obtain the time-dependent profiles $\langle n_i\rangle$ and the total penetrated flux given by Eq. (18). Let us start our discussion with the case $\Lambda=0$. In Fig. 3(a) we plotted the evolution of magnetic flux for $T^*=0.1$ and $n_{\rm ext}=400 \simeq n_B^*/2$. Time steps τ_k are chosen equidistant on a logarithmic scale. Clearly, as seen from Eq. (20), the evolution starts near the point $i=i_0$, where the initial profile $n_i^{(0)}$ departs from linearity. In a range of times $\tau<\tau^*$ a region $i_0(\tau)<i<N-i_0(\tau)$ remains free of flux, then shrinks, and finally vanishes at a characteristic time τ^*, where $i_0(\tau^*)=N/2$. Nearly linear profiles and slope discontinuities persist up to large times close to saturation. A plot of slopes $\langle n_{i-1}-n_i\rangle$ which are proportional to the current through the ith junction, is presented in Fig. 3(b). Note that flux profiles depicted in Fig. 3(a) have a slight positive curvature, which, however, remains small at any time.

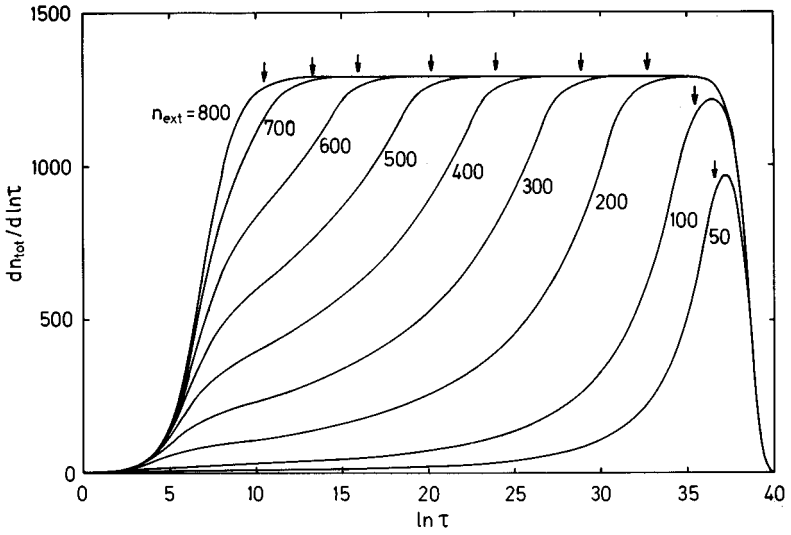

FIG. 5. ZFC creep rates within mean-field approximation for different external fields, where $\Lambda=0$, $\beta=100$, and $T^*=0.1$. The arrows indicate the time τ^* (see text).

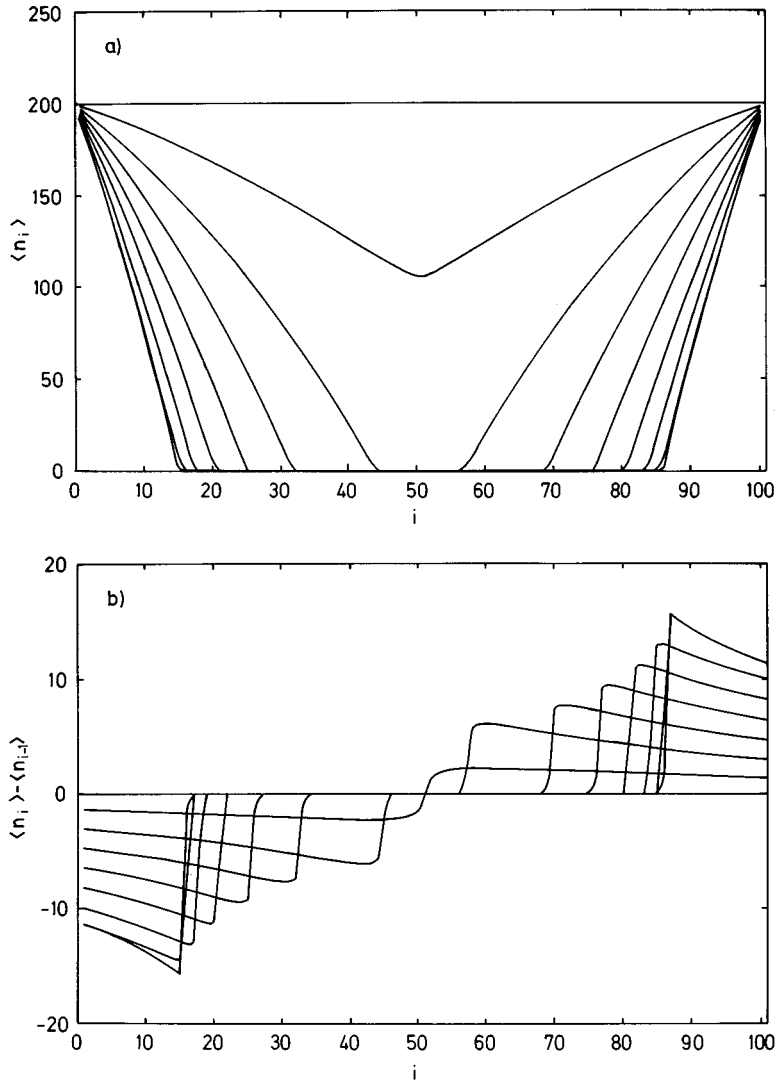

FIG. 6. Same as Fig. 3 but for $\Lambda=0.002$ (''Kim model'') and $n_{\rm ext}=200$. (a) Time evolution of a ZFC flux profile and (b) the corresponding slopes. Time steps are taken for $\ln \tau_k=(35/9)k$; $k=0,...,9$.

In the Appendix we present a simple calculation showing that under the assumption of linear profiles (i.e., neglect of that curvature) in the penetrated regions, the conventional logarithmic time dependence of the magnetization is obtained when two different regimes of the external parameters are considered. First, at sufficiently low temperatures, $T^*\ll 1$, and sufficiently small external fields, $n_{\rm ext}\ll n_B^*$, there is a range of times $\tau\ll\tau^*$, where the creep rate $S(\tau)=dn_{\rm tot}(\tau)/d\ln\tau$ becomes constant and is given by

$$S=2n_{\rm ext}^2T^*/\beta;\quad \tau\ll\tau^*. \tag{25}$$

Secondly, for strong fields of the order n_B^* or times $\tau>\tau^*$, again a constant creep rate can be defined after flux has penetrated the entire sample. In that case

$$S=\frac{N^2}{8\pi^2}\,\beta T^*;\quad \tau>\tau^*. \tag{26}$$

Numerical calculations shown in Figs. 4 and 5 essentially confirm these findings. For temperatures not too large a plateau in Fig. 4 emerges for $\tau>\tau^*$, whose height agrees with Eq. (26) and whose width expands with decreasing temperature. Calculations shown in this figure were performed for a fixed external field with $n_{\rm ext}=400\approx n^*/2$. The arrows in the figure indicate the time τ^*. On the other hand, data obtained for our lowest temperatures indicate the appearance of yet another plateau in the range $\tau\ll\tau^*$. This second plateau becomes more pronounced in cases of smaller fields, see Fig. 5, when the creep rate is small and proportional to $n_{\rm ext}^2$, in agreement with Eq. (25). For the lowest curve in Fig. 5(a) one can show that $n_{\rm tot}(\tau)$ varies only by a few percent in that range of times. Generally, however, for $T^*\gtrsim 0.1$ and $\tau<\tau^*$ we observe a nonlogarithmic relaxation. Saturation is reached after a time independent of $n_{\rm ext}$. Similar calculations were performed for the decay of remanent flux, with the general results $S_{\rm RM}(\tau)\simeq -S_{\rm ZFC}(\tau)$ apart from very short times.

Next we allow for a field dependence of the maximal Josephson current, in analogy to the Kim model, Eq. (22). Flux profiles and slopes in the case $\Lambda=0.002$ for $\beta=100$ and $n_{\rm ext}=200$ are displayed in Fig. 6 for a sequence of times τ_k. Contrary to Fig. 3, the profiles are concave for arbitrary times (apart from a small region around the symmetry point $i=N/2$). An experimental observation of profiles with negative curvature and their time evolution has recently been reported by Koblischka *et al.*[16] Creep rates $S(\tau)$ as a function of τ for the Kim model are plotted in Fig. 7(a) for different external fields. Beyond the time τ^*, creep rates are no longer

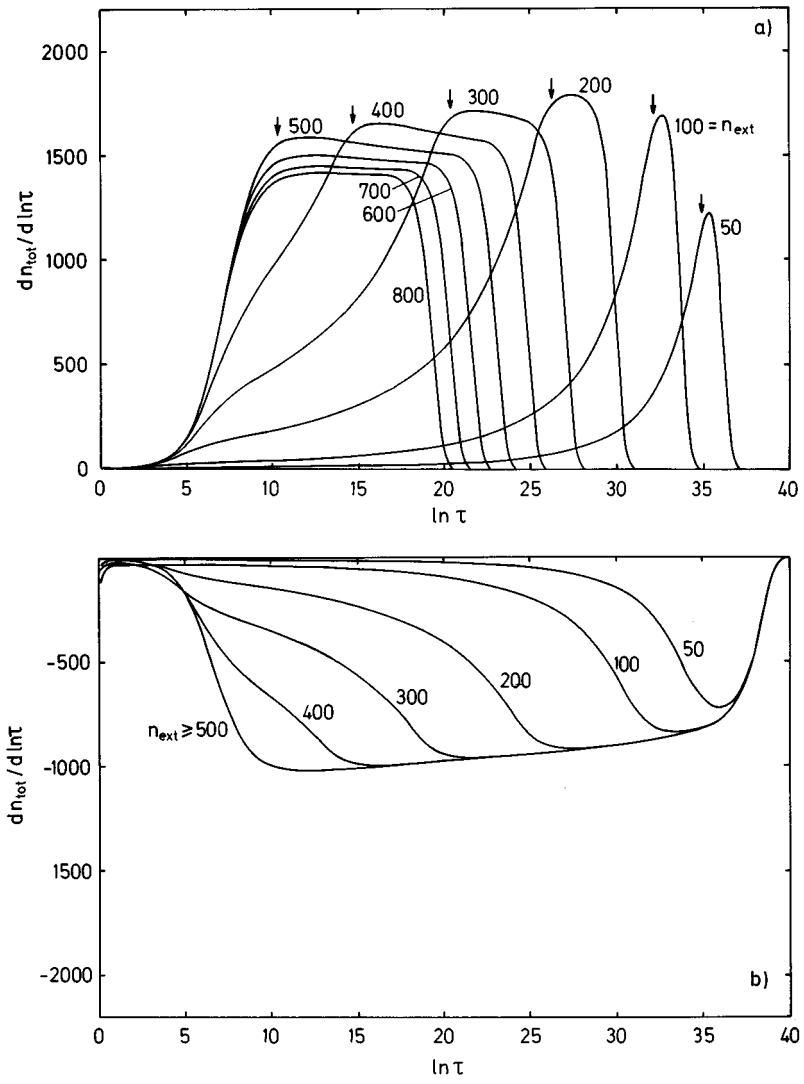

FIG. 7. Creep rates within mean-field approximation for different external fields, where $\Lambda=0.002$ (''Kim model''), $\beta=100$, and $T^*=0.1$ for (a) flux entering a zero-field-cooled sample and (b) decay of the remanent magnetization. The arrows indicate the time τ^* (see text).

constant but decrease slightly with increasing τ. For $\tau<\tau^*$, on the other hand, the curves are very similar to Fig. 5. In contrast to Fig. 5, however, saturation is now reached faster for higher fields in the ZFC case, whereas the final decay of the remanent flux remains unaffected by the field strength.

Some of the features displayed in Fig. 7 appear again to conform with recent experiments on high-T_c materials, although we have to keep in mind that the present model contains no spatial disorder effects. First, under ZFC conditions [Fig. 7(a)], a maximum creep rate is observed experimentally[19,26] and normally attributed to the time of full penetration τ^*, in accord to our findings. Secondly, at high fields $n_{\rm ext}>n^*$ and for a fixed observation time $\tau>\tau^*$ the creep rate drops by increasing the field in the ZFC case, whereas it stays constant in the RM case [Fig. 7(b)]. Such a behavior has recently been reported for Bi samples.[26]

The dependence of the ZFC creep rate on the external field $n_{\rm ext}$ (at a fixed observation time) is depicted in Fig. 8 together with experimental measurements.[35] For low fields the creep rate is nearly proportional to $n_{\rm ext}^2$, passes a maximum at intermediate fields, and decreases slowly at higher fields. Very similar experimental results were also reported by other authors.[18,35,36]

IV. MONTE CARLO SIMULATIONS

Our aim in this section is to perform dynamic Monte Carlo (MC) simulations of the master equation (15) in order to test the quality of results which were based on the mean-field approximation (19). From Eq. (13) it follows that the dominant transition rates near a critical state, and near equilibrium differ by a factor of the order $\exp(2/T^*)\gg 1$. Hence the stochastic process defined by the master equation (15) implies very different time scales, and the standard Metropolis algorithm will not be suitable in this case. Instead we shall employ a continuous-time MC procedure,[37,38] whose main steps are as follows: (i) calculate all $2N+2$ transition probabilities $W^{\pm}(n_i,n_{i-1})$ in the actual configuration $\{n_i\}$ at time τ ; (ii) put $r=\Sigma_i[W^+(n_{i+1},n_i)+W^-(n_i,n_{i-1})]$; select $\Delta\tau$ according to the probability distribution $P(\Delta\tau)=r\exp(-r\Delta\tau)$ and increase time by $\Delta\tau$; $\tau\rightarrow\tau+\Delta\tau$; (iii) select a transition according to probabilities $W^{\pm}(n_i,n_{i-1})/r$; and (iv) after performing this transition, return to (i).

Below we analyze some characteristic examples of the resulting magnetic relaxation in the ZFC case. In Fig. 9 the total magnetic flux in the sample, which was obtained from that algorithm, is plotted on a logarithmic time scale (full curves) and compared with the corresponding results of the

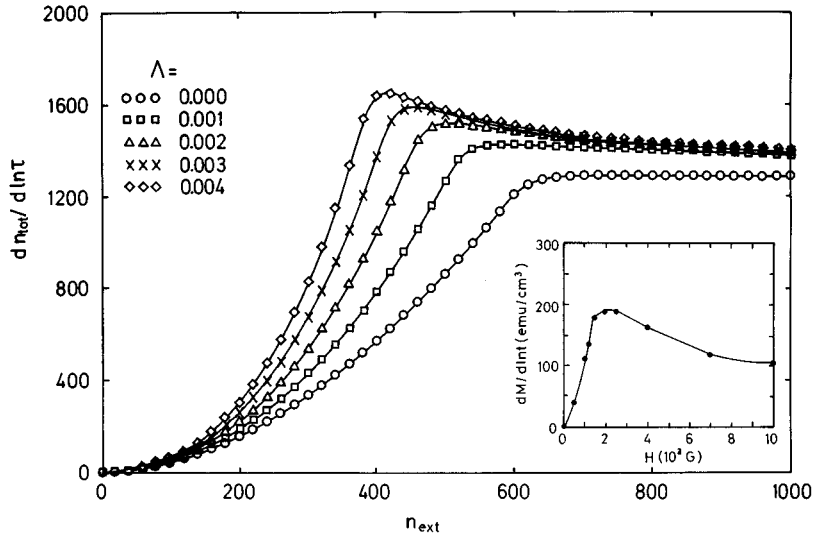

FIG. 8. ZFC creep rates as functions of $n_{\rm ext}$ for different values of Λ observed at $\ln\tau=15$, where $\beta=100$, $T^*=0.1$. Inset shows data for a single crystal of $Bi_2Sr_2CaCu_2O_x$ at $T=6$ K (Ref. 35).

mean-field (MF) approximation (dashed curves), using different temperatures. Other parameters were chosen as in Fig. 4. Note that both the MC and the MF method are based on exactly the same transition rates, given by Eq. (13), and this comparison therefore does not involve any adjustable parameter. In general, the simulation data when plotted against $\ln\tau$ show slightly faster relaxation than that predicted by the MF approximation, but evidently there is good overall agreement. By lowering the temperature, however, the simulated magnetic flux develops a wavy pattern which can be characterized as a sequence of ''avalanches,'' followed by plateaus of nearly constant flux. This behavior, which becomes clearly visible for $T^*\lesssim 0.025$ and which is absent in the MF results, is interpreted as follows. Inspection of the spatial dependence of the simulated flux right at the onset of a plateau shows that in general the flux density decreases linearly towards the interior of the system, e.g., for $i\leqslant i_0\leqslant N/2$ we have $n_i=n_{i-1}-\Delta n$, with some integer $\Delta n>0$. In these typical configurations only three different values of transition rates occur in the system, $W^{\pm}(n_i,n_i+\Delta n)=We^{\pm\alpha\Delta n}$ for arbitrary ''downhill'' or ''uphill'' transitions, respectively, and $W=W^{\pm}(0,0)=\nu\exp(-2/T^*)$ for spontaneous fluctuations in the nonpenetrated region. At low temperatures, the dominant rate is $\tilde{\tau}^{-1}=We^{\alpha\Delta n}$. Hence, after a time of the order $\tilde{\tau}$ a ''downhill'' transition will occur for some plaquette i, which increases the local slope $|n_i-n_{i-1}|$ and hence triggers subsequent faster transitions. This process shows up in Fig. 9 in plateaus of a length of about $\tilde{\tau}$ and a subsequent steep increase of the total flux, until a new linear flux profile is built, with Δn decreased by unity. Since the slope in the initial critical state corresponds to $\Delta n\simeq\beta/2\pi$, we expect about $\beta/2\pi$ ''avalanches'' until saturation is reached. From the same kind of reasoning we expect in the fully penetrated case ($\tau>\tau^*$) a difference in height of subsequent plateaus given by $\Delta n_{\rm tot}=N^2/4$. This is in fact confirmed by our MC calculations for the lower temperatures; also the length of plateaus agree with the above estimate for $\tilde{\tau}$. Clearly, such regular events would disappear, if structural disorder effects in our network were taken into account.

So far our description of magnetic relaxation was based on the mapping of our original equations of motion onto a master equation and therefore relied on condition (16). Clearly, this condition does not hold during an initial transient relaxation of the critical state, typically in a time do-

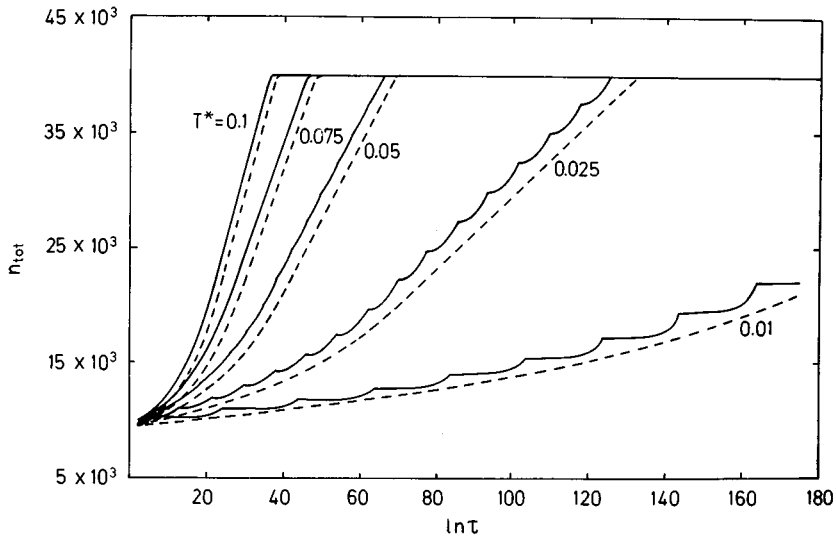

FIG. 9. Results of continuous-time Monte Carlo simulation (full lines) compared with the mean-field approximation results (dashed lines) for different temperatures; $\Lambda=0$, $\beta=100$, $n_{\rm ext}=400\approx n_B^*/2$. Statistical errors in the MC data are smaller than the line thickness.

main $\tau \lesssim 5$. Hence both our MC and MF data have no physical significance in that range. In order to justify our procedure for larger times, we have independently performed some Langevin dynamics simulations of the set of stochastic differential equations (7), starting out from a ZFC state, $\vartheta_i(t=0)=0$, and using $\Lambda=0$. As these simulations are rather time consuming, we only considered small systems ($N=10$) and a limited set of external parameters. Nevertheless, some interesting features emerged from these preliminary studies. On short time scales, given by t_{micro} (see Sec. II), we observe a fast and temperature-independent relaxation and the formation of a rather well-defined critical state with an almost linear flux profile, $|\vartheta_i-\vartheta_{i-1}|\approx\phi_{\mathrm{ext}}/\phi_0-\beta i$ in agreement with Eq. (9). As time proceeds, the relaxation becomes thermally activated. Calculated flux profiles nearly preserve their linearity, and hence justify our choice of initial conditions in the MC and MF calculations. Moreover, some Langevin-dynamics simulations on time scales up to $t\approx 10^7 t_{\mathrm{micro}}$ show sufficient overlap with our MC data to verify the creep rates during the early stages of the corresponding MC runs and the onset of ''avalanche'' effects. A more detailed discussion of Langevin-dynamics simulations will be presented elsewhere.

V. SUMMARY AND CONCLUSIONS

In cases of strong pinning $\beta\gg 1$, we derived a master equation describing thermally activated motions of magnetic flux quanta in a one-dimensional Josephson network. Magnetic fields due to the currents induced in the system were taken into account by self-inductance coefficients. The mean-field approximation to solutions of the master equation allowed us to follow magnetic relaxation phenomena up to very long observation times for different temperatures and external field values. Assuming the widely used Kim-model description for the relation between the local values of magnetic field and critical current, our calculations reproduce several flux-creep phenomena similar to those recently observed in samples of type-II superconductors with very short coherence lengths. In particular, we obtained logarithmic or nonlogarithmic flux-creep phenomena depending on temperature and the applied field, in good qualitative agreement with experimental findings. Numerical simulations confirm the applicability of the mean-field approximation to the cases considered in this paper.

ACKNOWLEDGMENTS

This work was supported in part by the Polish State Committee for Scientific Research, Grants No. 203439101 and C/3429/94, and by the Bundesministerium für Wissenschaft und Forschung, Project No. X083.6.

APPENDIX: CONTINUUM LIMIT

Let us assume here that $\langle n_i\rangle$ as determined by Eq. (20) varies on a length scale much larger than the lattice constant a. Then we can perform a continuum limit $i\to s=x/a$, $m_i(\overline{\tau})\to m(s,\overline{\tau})$, $f_i-f_{i-1}\to\partial f/\partial s$, where we have defined $m_i=\alpha\langle n_i\rangle$ and $\overline{\tau}=\alpha\tau\exp(-2/T^*)$. Using Eq. (20) we obtain a nonlinear diffusion equation for $m(s,\overline{\tau})$

$$\frac{\partial m}{\partial\overline{\tau}}=2\frac{\partial}{\partial s}\left[\sinh\left(\frac{\partial m}{\partial s}\right)\right]. \tag{A1}$$

Temperature and the external flux enter Eq. (A1) only via the initial and boundary conditions. Phenomenological diffusion equations of a similar type have been discussed earlier to describe flux creep phenomena in hard superconductors.[29,31,39,40] Integration of Eq. (A1) from $s=0$ to N under the assumption of initial conditions symmetric with respect to $s=N/2$ yields

$$\frac{d}{d\overline{\tau}}m_{\mathrm{tot}}=-4\sinh\left[\frac{\partial m}{\partial s}\,(s=0,\overline{\tau})\right], \tag{A2}$$

where $m_{\mathrm{tot}}(\overline{\tau})=\int_0^N m(s,\overline{\tau})ds$ is proportional to the total number of flux quanta in the system. The numerical results presented in Sec. III show that the curvature of the flux profiles (in the case $\Lambda=0$) remain negligible during the whole relaxation process, so the assumption of nearly linear profiles for arbitrary times will be a good approximation to our problem. Assuming $\partial m/\partial s=\Delta_0(\overline{\tau})$ to be spatially constant in the penetrated region, we easily obtain a relation between $\Delta_0(\overline{\tau})$ and the total flux in the network.[31] In the following we restrict ourselves to a ZFC system and distinguish between a fully and a partially penetrated system. For a fully penetrated system, $0\leqslant\Delta_0(\overline{\tau})\leqslant 2m_{\mathrm{ext}}/N$, the total flux depends linearly on $\Delta_0(\overline{\tau})$,

$$m_{\mathrm{tot}}(\overline{\tau})=Nm_{\mathrm{ext}}-\frac{N^2}{4}\,\Delta_0(\overline{\tau}), \tag{A3}$$

where $m_{\mathrm{ext}}=\alpha n_{\mathrm{ext}}$. Eliminating $\Delta_0(\overline{\tau})=\partial m/\partial s(s=0,\overline{\tau})$ from Eqs. (A2) and (A3), we arrive at an ordinary differential equation for the total flux which holds in the range $Nm_{\mathrm{ext}}\geqslant m_{\mathrm{tot}}\geqslant Nm_{\mathrm{ext}}/2$:

$$\frac{dm_{\mathrm{tot}}}{d\overline{\tau}}=4\sinh\left[\frac{4}{N^2}\,(Nm_{\mathrm{ext}}-m_{\mathrm{tot}})\right]. \tag{A4}$$

This equation has the same structure as the equation discussed by Nieuwenhuizen and Pankert[15] for a single superconducting loop, but takes into account system size effects through a dependence on N. Equation (A4) is fulfilled by

$$m_{\mathrm{tot}}(\overline{\tau})=Nm_{\mathrm{ext}}-\frac{N^2}{4}\ln\left\{\frac{1+e^{-x_0}\tanh[(8/N^2)\overline{\tau}]}{\tanh[(8/N^2)\overline{\tau}]+e^{-x_0}}\right\}, \tag{A5}$$

with $x_0=(4/N^2)[Nm_{\mathrm{ext}}-m_{\mathrm{tot}}(\overline{\tau}=0)]$. For a range of times $\exp(-x_0)\ll(8/N^2)\overline{\tau}\ll 1$ the total flux shows a logarithmic dependence on time. The corresponding constant creep rate is $dm_{\mathrm{tot}}/d\ln\tau=N^2/4$ and is equivalent to Eq. (26).

Now we want to consider a partially penetrated ZFC system $\Delta_0(\overline{\tau})>2m_{\mathrm{ext}}/N$. In this case the relation between the total flux and the linear slope of the profile is given by (cf. Ref. 31)

$$m_{\mathrm{tot}}(\overline{\tau})=\frac{m_{\mathrm{ext}}^2}{\Delta_0(\overline{\tau})}. \tag{A6}$$

Together with Eq. (A2) we can again eliminate $\Delta_0(\tau)$, and in analogy to the fully penetrated case we get an ordinary differential equation which holds in the range $0 \leqslant m_{\rm tot} \leqslant N m_{\rm ext}/2$:

$$\frac{dm_{\rm tot}}{d\overline{\tau}} = 4 \sinh \frac{m_{\rm ext}^2}{m_{\rm tot}}. \tag{A7}$$

Under the assumption that changes in the magnetization are small—that means $\Delta m = m_{\rm tot} - m_{\rm tot}(0) \ll 1$—we can expand $1/m_{\rm tot}(\overline{\tau})$ about $1/m_{\rm tot}(0)$ in Δm. In this way we get a differential equation for Δm of the same structure as Eq. (A4). For intermediate times we again arrive at a nearly constant creep rate, which is given now by Eq. (25).

[1] K. A. Müller, M. Takashige, and J. Bednorz, Phys. Rev. Lett. **58**, 1143 (1987).
[2] G. Deutscher and K. A. Müller, Phys. Rev. Lett. **59**, 1745 (1987).
[3] I. Morgenstern, K. A. Müller, and J. G. Bednorz, Z. Phys. B **69**, 33 (1987).
[4] V. L. Aksenov and S. A. Sergeenkov, Physica C **156**, 18 (1988).
[5] D. A. Huse and S. Seung, Phys. Rev. B **42**, 1059 (1990).
[6] Ying-Hong Li and S. Teitel, Phys. Rev. Lett. **66**, 3301 (1991).
[7] W. Xia and P. L. Leath, Phys. Rev. Lett. **63**, 1428 (1989); Phys. Rev. B **44**, 9619 (1991).
[8] R. de Luca, S. Pace, and B. Savo, Phys. Lett. A **154**, 185 (1991).
[9] G. Parodi and R. Vaccarone, Physica C **173**, 56 (1991).
[10] A. Majhofer, T. Wolf, and W. Dieterich, Phys. Rev. B **44**, 9634 (1991).
[11] T. Wolf and A. Majhofer, Phys. Rev. B **47**, 5383 (1993).
[12] D. Reinel, W. Dieterich, T. Wolf, and A. Majhofer, Phys. Rev. B **49**, 9118 (1994); Physica C **245**, 193 (1995).
[13] J. R. Phillips, H. S. van der Zant, J. White, and T. P. Orlando, Phys. Rev. B **47**, 5219 (1993).
[14] D. Dominguez and Jorge V. José, Phys. Rev. Lett. **69**, 514 (1992).
[15] Th. Nieuwenhuizen and J. Pankert, Europhys. Lett. **11**, 457 (1990).
[16] M. R. Koblischka, Th. Schuster, B. Ludescher, and H. Kronmüller, Physica C **190**, 557 (1992).
[17] Y. Yeshurun and A. P. Malozemoff, Phys. Rev. Lett. **60**, 2202 (1988).
[18] Y. Yeshurun, A. P. Malozemoff, F. Holtzberg, and T. R. Dinger, Phys. Rev. B **38**, 11 828 (1988).
[19] P. Svedlindh, K. Niskanen, P. Norling, P. Nordblad, L. Lundgren, C. Rossel, M. Sergent, R. Chevrel, and M. Potel, Phys. Rev. B **43**, 2735 (1991).
[20] A. Spirgatis, R. Trox, J. Kötzler, and J. Bock, Phys. Rev. Lett. **67**, 3444 (1991).
[21] D. E. Lacey and J. A. Wilson, Supercond. Sci. Technol. **5**, 724 (1992).
[22] C. W. Hagen and R. Griessen, Phys. Rev. Lett. **62**, 2857 (1987); in *Studies of High Temperature Superconductors*, edited by A. Narlikar (Nova Science, Commack, NY, 1989).
[23] M. V. Feigel'man, V. B. Geshkenbein, A. I. Larkin, and V. M. Vinokur, Phys. Rev. Lett. **63**, 2303 (1989).
[24] M. Feigel'man, V. B. Geshkenbein, and A. T. Larkin, Physica C **167**, 177 (1990).
[25] M. A. P. Fisher, Phys. Rev. Lett. **62**, 1145 (1989).
[26] P. Svedlindh, C. Rossel, K. Niskanen, P. Norling, P. Nordblad, L. Lundgren, and G. V. Chandrashekhar, Physica C **176**, 336 (1991).
[27] H. Risken, *The Fokker-Planck Equation* (Springer-Verlag, Berlin, 1989).
[28] N. G. van Kampen, *Stochastic Processes in Physics and Chemistry* (North-Holland, Amsterdam, 1981).
[29] P. W. Andersen and Y. B. Kim, Rev. Mod. Phys. **36**, 39 (1964).
[30] M. R. Beasley, R. Labusch, and W. W. Webb, Phys. Rev. **181**, 682 (1969).
[31] H. G. Schnack, R. Griessen, J. Lensink, C. J. van der Beek, and P. H. Kes, Physica C **197**, 337 (1992).
[32] Y. B. Kim, C. F. Hempstead, and A. R. Strnad, Phys. Rev. **129**, 528 (1963).
[33] V. Ambegaokar and A. Baratoff, Phys. Rev. Lett. **10**, 486 (1963).
[34] V. Ambegaokar and B. I. Halperin, Phys. Rev. Lett. **22**, 1364 (1969).
[35] D. Shi, A. Umezawa, and R. F. Fox, Phys. Rev. B **42**, 2062 (1990).
[36] A. Umezawa, S. K. Malik, G. W. Crabtree, H. H. Wang, L. K. Montgomery, K. D. Carlson, and J. M. Williams, Physica C **185–189**, 2665 (1991).
[37] K. Binder, in *Monte Carlo Methods in Statistical Physics*, edited by K. Binder, Topics in Current Physics Vol. 7 (Springer-Verlag, Berlin, 1979).
[38] D. Bedeaux, K. Lakatos-Lindenberg, and K. E. Shuler, J. Math. Phys. **12**, 2116 (1971).
[39] C. J. van der Beek, G. J. Nieuwenhuys, and P. H. Kes, Physica C **197**, 320 (1992).
[40] V. Calzona, C. Rizzuto, and A. S. Siri, Supercond. Sci. Technol. **6**, 46 (1993).